RSC Advances

ROYAL SOCIETY OF CHEMISTRY

www.rsc.org/advances

Journal Name

ARTICLE

A region-selective modified capillary microfluidic device for fabricating water-oil Janus droplets and hydrophilic-hydrophobic anisotropic microparticles

Ke Xu‡, Xue-Hui Ge‡, Jin-Pei Huang, Zhu-Xi Dang, Jian-Hong Xu*, Guang-Sheng Luo

Here we developed a novel and facile microfluidic approach to produce W-O Janus droplets with broadened operation range (lower Ca number and higher volume ratio of two dispersed phases) , and then fabricate Hydrophilic-Hydrophobic Anisotropic Janus Particles (HHAJP). The volume ratio of two dispersed phases and the exposure area of specific phase could be adjusted by controlling the surfactant concentration in continuous phase and the volume flow ratio of two liquids. The anisotropic microparticles could distribute on the oil-water interface orderly and stably, indicating its potential applications as interface stabilizer and phase transfer catalyst.

INTRODUCTION

Anisotropic functional particle is particle material that integrated different functions on different sides, and it has been noticed recently for fields such as multi-phase catalyst[1, 2], optical pixel unit[3-7], targeted drug release[8-12] and emulsion stabilizer[13, 14]. In these fields, the synergy of different functions enhances and broadens the applications of particles significantly.

Emulsion droplets are traditionally used as templates of micro-particle materials. For example, researchers have fabricated microbeads with different surface topographies from single-phase droplets[15-18], core-shell microcapsules with single and multiple cores from W/O/W or O/W/O double emulsion droplets[12, 19-23], micro-bubbles covered by gel-film from G/W/O or G/O/W double emulsion droplets[24-26], and more complicated microparticles from more complicated multiple emulsion droplets[21, 27]. Janus emulsion droplets (Janus droplets) are naturally templates for anisotropic particles. When the interfacial tensions in a tri-phase emulsion system with 1 continuous phase and 2 dispersed phases satisfies certain relationship, the two dispersed phase droplets would connected with each other and then form an integral 'Janus Droplets'[28, 29]. After solidification process, such Janus droplets would become anisotropic particles. By numerical calculation, researchers have alleged that the volume-ratio and exposure area ratio of the two faces could be controlled by changing the liquid volume ratio and adjusting the interfacial tension relationship, so the structure of two faces could be controlled[30, 31].

Traditionally, Janus droplets are produced by simply stirring three immiscible phases[32-34], but such process could hardly control the uniformity of products. Recently, microfluidic method has been used to realize highly controllable and mono-dispersed generation of emulsion droplets[18, 35-37], especially droplets with complicated structure[12, 19, 20, 24, 25, 38, 39]. Some approaches have shown significant progress to produce uniform Janus droplets in microfluidic devices[40]. Researchers produced engulfing structure droplets with double-capillary method firstly, with Janus-stable fluid system, and then the inner droplet could breakout and contact with the continuous phase, forming a Janus structure[40-42]. However, the dynamic process for the inner droplet to contact with the continuous phase is not controllable and may be extraordinary long if the middle phase has high viscosity (e.g. polymer solution or nanoparticle suspension). So some researchers developed a more controllable in-situ method, by forming a parallel laminar flow of two dispersed phases at upstream and then cutting the dual-phase laminar flow into Janus droplet with continuous phase[43]. This in-situ method is much more controllable to produce uniform Janus droplets, and then to get anisotropic particles. It has been used to synthesize anisotropic catalyst and medical application[10, 44].

However, this in-situ method requires spontaneous & stable laminar flow after two dispersed phases converging, so the operation condition has to be limited with: 1) Relatively high Capillary number (Ca), e.g. low interfacial-tension between dispersed phases with relatively high total flow rates;

The State Key Lab of Chemical Engineering, Department of Chemical Engineering, Tsinghua University, Beijing 100084, China. E-mail: xujianhong@tsinghua.edu.cn . Tel: +86-10-62773017. Fax: +86-10-62773017.
‡ These authors contributed equally.
† Electronic Supplementary Information (ESI) available. See DOI: 10.1039/b000000x/

2) considerably limited volume ratio of the two dispersed phases. Such limits in two-phase system has been analysed by researchers[45]. Consequently, the current application of this method is restricted in generating O-O Janus droplet (with interfacial tension less than 1mN/m), because the interfacial tension of W-O system is always relatively high (> 4 mN/m) that one phase would always break up and then be cut by the other phase into droplets or plugs, which prevents its application as phase transfer catalyst and as surface-stabilizer. Even for O-O Janus generation, researcher could only realize the volume ratio of two phases between 1:5~5:1.

Here in this work, we present an essential improvement of the in-situ method to produce water-oil Janus droplets, with a Region-Selective Modification (RSM) of the microchannel. By changing the wettability of selected region on microchannel wall, the interaction between certain liquid and the selected region surface would be adjusted. We adjusted the region surface to have higher wettability difference to the two dispersed fluids. Then the two fluids formed paralleled co-laminar flow in the selected region and intend to stick on till the continuous phase cutting them into Janus droplets. By applying the RSM approach for the in-situ method, we successfully expanded the in-situ method to the systems with relatively higher interfacial tension (from ~1mN/m in previous work to >6 mN/m in this work (γ_{EW} =6.13mN/m)) and larger volume-ratio range (from 1:5~5:1 in previous work to 1:10~40:1 in this work), and lower Capillary number (from 10^{-2}~10^{-1} in previous work to 10^{-4}~10^{-1} in this work) [46, 47]. Thus, we could operate the W-O system in stable laminar flow in much broadened operation range. With tolerance of higher interfacial tension, we could generate W-O Janus droplet in-situ, and then fabricate Hydrophobic-Hydrophilic Anisotropic Janus Particles (HHAJP). Furthermore, we find that the volume ratio of the two dispersed phase and the exposure area ratio of specific phase in the particle could be modified easily by simply adjusting the flow rates ratio of liquids as well as surfactant concentration in continuous phase.

EXPERIMENTAL SECTION

Microfluidic device and Materials

Here we use a two-stage capillary microfluidic device. The dispersed and continuous channels are micro-capillaries crossing in a square 20 mm long ×20 mm wide × 3 mm high polymethyl methacrylate (PMMA) chip. There are two capillaries used here, the first one flow the dispersed phases in which inner wall is applied RSM approach and the second one flow the continuous phase to shear the Janus droplet in the tip. They all insert into the channels in the PMMA chip with 1.50mm wide × 1.50 mm high to assure their coaxality. The diameter of capillaries is 1.5 mm(O.D) ×1.05mm(I.D). The first capillary is tapered using a micropipette puller(P-97, SUTTER Co.Ltd., USA) to form a tip with approximately a diameter of 200 μm. The two dispersed phases are injected through micro-needles with inner diameter of 160 μm and outer diameter of 340μm. And one needle which flow the water phase is placed

to touch inner wall of first capillary and near the tip (less than 2 mm to the tip) while the other one which flow the oil phase is in the upper middle of the capillary and far away from the tip (more than 30 mm to the tip) thus water phase would stick to the wall as soon as it flows out while oil phase would have enough time to form stable laminar flow, thus when the two phases converges, they would flow paralleled through the tip to be sheared to Janus droplets. Microsyringe pumps (LSP01-1B, Baoding Longer Precise Pump Co. Ltd) are used to pump fluidic devices. Typical orders of magnitude of two dispersed phases and continuous phase are 10 μL min^{-1} and 1000μL min^{-1}, respectively.

We used two sets of fluids in the device, one for modification and the other for forming W-O Janus droplet. The modification system concludes fluids of aqueous with 20 wt.% NaOH and 2.0 wt.% Tween 80(surfactant), normal octane with 2 wt.% Span 80(surfactant), liquid paraffin with 5 wt.% Span 80(surfactant) and hexamethyldisiloxane .

The system to form W-O Janus droplet and the HHAJPs is composed of deionized water with 10 wt.% Poly(ethylene glycol) diacrylate monomer (PEGDA) and 0.5wt.% HMPF (photo initiator), liquid paraffin with 0.05~2.0 wt.% Span80 (surfactant, the mass concentration changed when needed), and the Photo-curing material ethoxylated tri methylolpropane triacrylate monomer(ETPTA) with 0.5wt.% HMPF (photo initiator). For both above conditions, the needle closer to the tip flow water phase while the other needle far away from the tip flow the oil phase. **Table 1** shows the interfacial tensions of different systems.

Table 1 The interfacial tensions of different systems

Mass fraction of Span80(w%)	γ_{EW} (mN/m)	γ_W (mN/m)	γ_E (mN/m)
0.05	6.13	4.89	3.47
0.1	6.13	4.34	3.49
0.15	6.13	4.27	3.5
0.5	6.13	4.12	3.53
1	6.13	3.77	3.48
2	6.13	2.71	3.47

Torza and Mason [46, 47] used spreading coefficient (S_i) to predict the morphology of three fluids, as follows,

$$S_i = \sigma_{jk} - (\sigma_{ij} + \sigma_{ik}) \quad (\ i \neq j \neq k = 1,2,3\ ) \quad , \quad \sigma_{jk}$$

represent the interfacial tension bewteen j and k fluids.

$S_1 < 0 \quad S_2 < 0 \quad S_3 > 0$, engulfing structure

$S_1 < 0 \quad S_2 < 0 \quad S_3 < 0$, Janus structure

$S_1 < 0 \quad S_2 > 0 \quad S_3 < 0$, separating structure

Here in our work, the interfacial tensions of three fluids are diverse because we use continuous phase with different mass fraction of surfactant. We used all data to calculate the Spreading coefficient, we could obtain as the following **Table 2**. It shows that we can produce W-O Janus droplet with different structures by using these systems.

**Table 2** The spreading coefficients of different systems

Mass fraction of Span80(w%)	S_1	S_2	S_3
0.05	-7.55	-2.23	-4.71
0.1	-6.98	-1.7	-5.28
0.15	-6.9	-1.64	-5.36
0.5	-6.72	-1.52	-5.54
1	-6.42	-1.12	-5.84
2	-5.37	-0.05	-6.89

Generated Janus droplets could be polymerized and solidified into ETPTA and hydrogel composed of PEGDA under UV point light source (LC8, Model L9588-01,Hamamatsu) exposure in l0 seconds. ETPTA is hydrophobic while hydrogel is hydrophilic, thus we obtained the HHAJPs. The chemicals used are chemically pure and purchased from Bai Ling Wei and Sigma corporations.

We used optical microscope (BX61, Olympus) assembled with high speed camera (DK-2740, Dantech) to take micro-photographs and movies. And we used dynamic interfacial tension measurement instrument (OCAH200, DataPhysics Instruments GmbH, Germany) to utilize the pendant drop method and the contacting angle method to measure the interfacial tension of experiment systems and the contact angle of capillary inner wall before and after hydrophilic modification. We also used SEM to observe the surface of the wall to find the mechanism of modification.

Region-Selective Modification Process

Here we propose a novel RSM process and then to construct parallel hydrophobic-hydrophilic pathways for the two inner phases. **Scheme** 1 shows the process step by step. First, we place the two needles to the separate position as the **Scheme** 1.1 shows and then immerse the micro-device into hexamethyldisiloxane for 5 hours in 80℃ atmosphere to make the capillary overall hydrophobic and ETPTA-wetting. Secondly, aqueous solution containing NaOH and surfactant is injected through the needle touching the inner wall after oil phase flow through the other needle and occupy the channel. With high flow rates of both liquids, which leads to a high Ca condition, we form a steady co-laminar flow in the dispersed-phase tube. After continuously flowing for 5 hours, NaOH reacts with the capillary wall and makes the contacting region water-wetting while remaining the rest region ETPTA-wetting. Thirdly, we stop flowing the modification fluids and obtain a selective region to be hydrophilic (the blue region in **Scheme** 1.3) while other parts remain hydrophobic. Thus, we inject Janus formation fluids, i.e. water and ETPTA. Because of the difference in wettability of inner wall towards water and ETPTA, we obtain two parallel pathways for aqueous phase and ETPTA phase respectively and they would be sheared simultaneously at the tip by continuous phase fluid. That is how we obtain W-O Janus droplets by in-situ method after RSM.
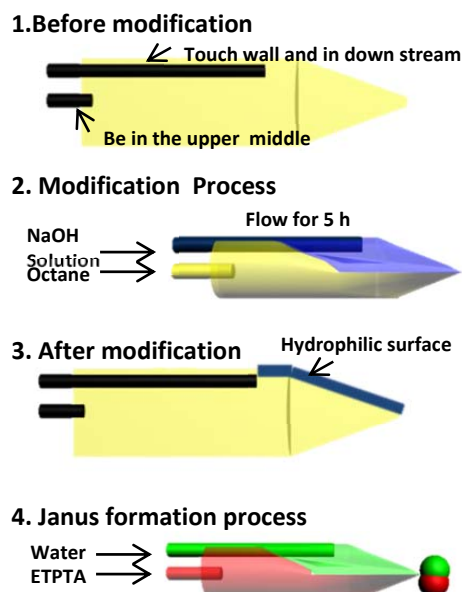

Scheme 1. A brief scheme of the RSM process step by step. 1) Capillary assembly We put two needles into the micro-capillary as the dispersed phase channels and modified the overall capillary into hydrophobic and ETPTA-wetting.2) Modifier injection. Aqueous solution containing NaOH and surfactant is injected in through a needle touching the inner wall after oil (octane) occupying the channel with high flow rates of both liquids to form a steady co-laminar flow in the dispersed-phase tube. This modification process last for 5 hours. 3) After RSM. We obtain a selective region (the blue region) to be hydrophilic while other parts remain hydrophobic. 4) Generating Janus droplets. Working system which are water phase and ETPTA are injected into the device after RSM process to form stable paralleled laminar flow and to be sheared at the tip by continuous phase to form Janus droplet.

RESULTS AND DISCUSSIONS

#### Modification result of capillary inner wall

After modification, the wettability of inner channel wall has been adjusted. A water-wetting pathway is formed on the ETPTA-wetting capillary wall from the aqueous phase needle tip to the capillary orifice. Then we compare the contact angle between water and inner wall before and after NaOH solution modification. First, we modify two glasses to hydrophobic using the same method as **Scheme** 1.1 shows and one using NaOH solution to modify to hydrophilic and the other doesn't. Then we measure the contact angles of water droplet on the two glasses based in ETPTA atmosphere. The comparison result is shown in **Fig.** 1b, where we find the contact angle is 169.9° on ETPTA-wetting glass (glass only modified by hexamethyldisiloxane) and 52.1° on hydrophilic glass (glass first modified by hexamethyldisiloxane and then by NaOH aqueous solution), which means the raise in the hydrophilic wettability. The SEM pictures shown in **Fig**. 1c and 1d indicate that the glass surface is considerably modified, full of ravine due to NaOH solution corroding. In experiments, we found th modification would maintain effective for more than 10 days.
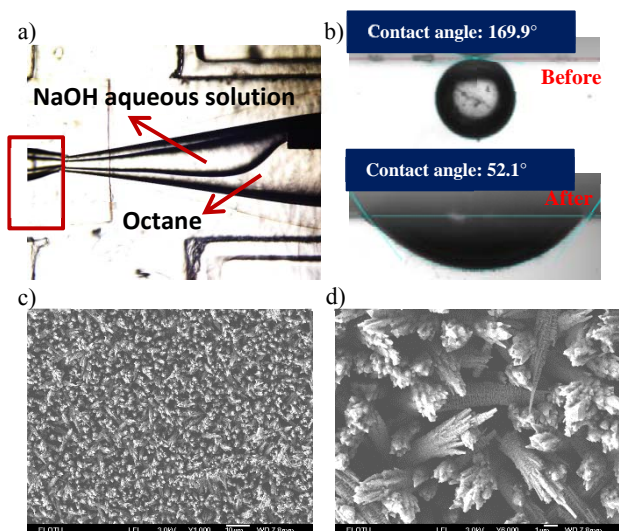
Fig. 1 The microscopic photograph of hydrophilic modification process and the modification effect comparison. a) The microscopic photograph of hydrophilic modification process. The NaOH and octane formed co-laminar flow in the dispersed tube. The red square is the colleting tube to invent the NaOH aqueous solution to interact with the continuous tube. It just exist temporarily in this step. b) The comparison of contact angles between capillary and water in ETPTA monomer before (169.9°) and after hydrophilic modification (52.1°). c) and d) the SEM pictures of the glass surface after modification. d) the magnification of specific part of the surface. The surface is eroded severely by the NaOH aqueous solution. The black bar represents as 200 μm.

Formation of Droplets

The schematic diagram of synthesis process of Janus emulsion droplets and particles is shown in **Scheme** 1.4. In the microfluidic device after RSM process, we formed stable and controllable Janus emulsions. A movie of Janus droplets formation is in supporting material (Movie S1-formation process).
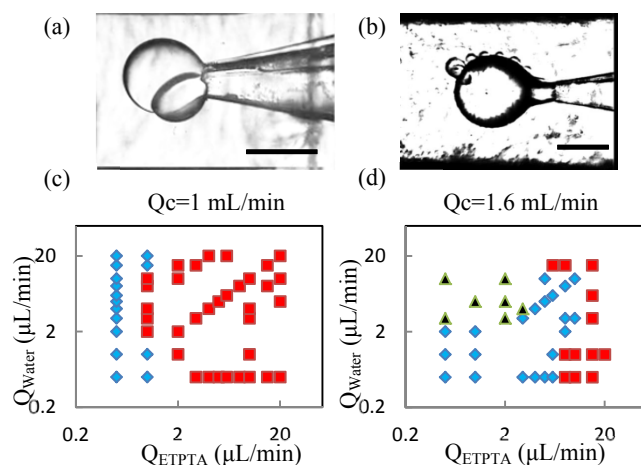

Fig.2 The microscopic photos of the synthesis of mono-dispersed Janus droplets a) Janus droplet formation process. Oil and water phase formed co-laminar flow and adhered together to flow out the tip, then the integral drop grow bigger until to be sheared down from the tip to form a Janus droplet. b) The colourful Janus droplet. The red part represents oil phase (ETPTA) and the colourless

phase represents water phase. c) Janus particles after solidification. They are monodispersed. The scale bars above represent 500 μm

The growing, cutting and flowing process is shown in **Fig.** 2a. If we solidify the generated Janus droplets in-situ under UV exposure, we could get HHAJPs. **Fig.** 2b and 2c show the Janus droplet in the channel and Janus particles after solidification, which we could find those HHAJPs are highly monodispersed.

During the formation process, we research on the flow rates range to form stable Janus droplet. If ETPTA and water fluids form a parallel co-laminar flow and are sheared by continuous phase to form one water semi-sphere droplet sticking to one ETPTA semi-sphere droplet. We call this Janus droplet as "single Janus droplet" as shown in **Fig.** 3a. Apart from this, we observe another stable flowing pattern. When the two phases stay longer in the tip while the flow rate of water phase is high, there would be multiple water droplets formed and stuck one ETPTA droplet, forming multiple Janus structure, we called that "Multiple Janus" as shown in **Fig.** 3b. Here in this work, we focus on the single Janus droplet.
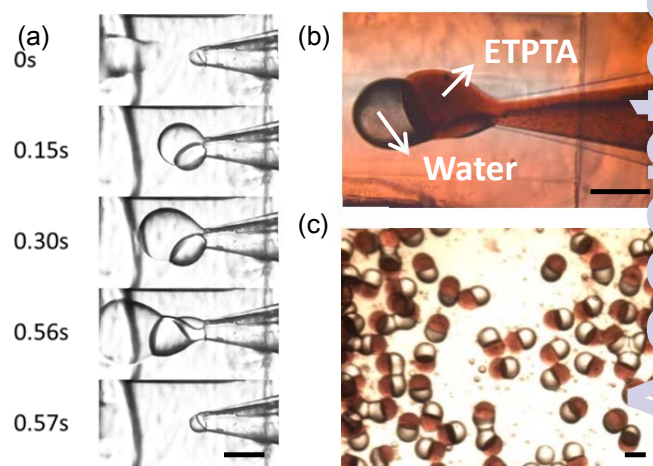

Fig.3. The two flow patterns of Janus droplet: single Janus and multiple Janus and their formation condition. a) Single Janus. One water and one ETPTA droplet form together. b) Multiple Janus. Many small water droplets adhere to one ETPTA droplet. c) and d) the relationship between Janus structure and the flow rates in different flow rates of continuous phase. Red squares represent multiple Janus is formed in the corresponding flow rates, blue rhombus represent rates single Janus is formed in the corresponding flow, black triangle represent an unstable state which it swing between single Janus and multiple Janus. The black bars represent 500 μm.

So we explore the relationship between the two Janus structures and the flow rates to find out the flow rates scope to form stable single Janus. Fixing the continuous flow rates as 1 mL/min and 1.6 mL/min, we change the flow rates of the ETPTA and water phases. The results show that a relatively higher continuous flow rate could help to avoid multiple Janus droplets, as shown in **Fig.** 3c and **Fig.** 3d.

Enlargement of the operation range

The operation range of our RSM method is considerably enlarged compared with previous in-situ method without RSM, because the RSM reduces the difficulty to get stable laminar flow in dispersed-phase channel. Both the restrictions in interfacial tension and in volume ratio are reduced considerably. The flow rate in the dispersed-phases channel could be operated in a 2-order lower Ca condition than the previous work. The volume ratio of the two dispersed phases is also extended considerably. **Table 3** and **Fig.** 4 show the comparison between our work and previous work. To elaborate our work's advantage more clearly, we quote the picture from the reference[43] in **Fig.** 4b and analyse our data in the same way to find the enlargement. The blue circles region represent that we could obtain stable Janus droplet in the corresponding Ca number. From the comparison, we find that we could produce stable droplets in a lowest Ca number equal to 0.0001, while in the reference, it could only form stable droplet when the Ca number was more than 0.01, which show our significant improvement in the Ca number. Thus we could synthesis in lower flow rates and higher interfacial tension. This improvement allows us to produce HHAJPs composed of water and oil phase (which would have higher interfacial tension) and larger flow rates range (from low flow rates to high rates).
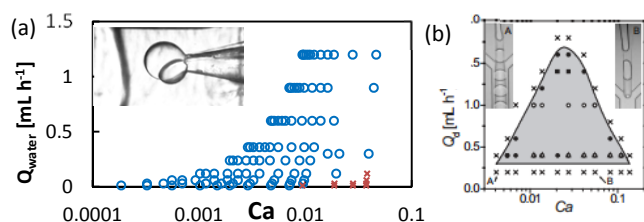
Fig. 4 The comparison of Ca number range between our work and previous work to show the enlargement of operation range in our work. a) the relationship with the flow rates to Ca number in our work. The blue circle represents stable single droplet, and the red cross represents unable droplet. It represent the stable range of Ca number varies from 0.0001 to 0.01. b) the citation of previous work as comparison[43]. The stable range of Ca number here was from 0.01 to 0.1.

Table 3 the comparison of operation range of this work and previous work.

	Unmodified[43, 44]	Modified
Interfacial tension	< 1mN/m	6mN/m
Inner phase ratio	0.2~5	0.1~40
Ca Number	10^{-2}~10^{-1}	10^{-4}~10^{-1}

Precise control on the Janus droplets' size and structure

Moreover, we could control the size and structure of the Janus droplets precisely by adjusting the flow rates and changing the interfacial tension. **Fig.** 5 show the structure change of Janus emulsion when flow rates ratio of two phases changes. They are all Janus particles but have different volume ratio of hydrophilic semi-sphere to hydrophobic semi-sphere. **Figs.** 5a~5c are the micrographs when the flow rates ratio of water to ETPTA arise from 1:10 to 10:1. We can see that when the flow rates of two phases are the same, the semi-sphere of

each phase almost have the same volume. Actually, the ratio is not 1:1 and it has relationship to the interfacial tensions of three phase[31], because of the deformation between two dispersed phases when they touched. Here we ignore the influence of the deformation and assume the dispersed phase as spherical crown, we find that the diameter ratio of two spherical crowns raise along the increase of the flow rates ratio as shown in **Fig.** 5d. Through the relationship, we could adjust the size of each part of the HHAJPs by adjusting the flow rates of each phase.
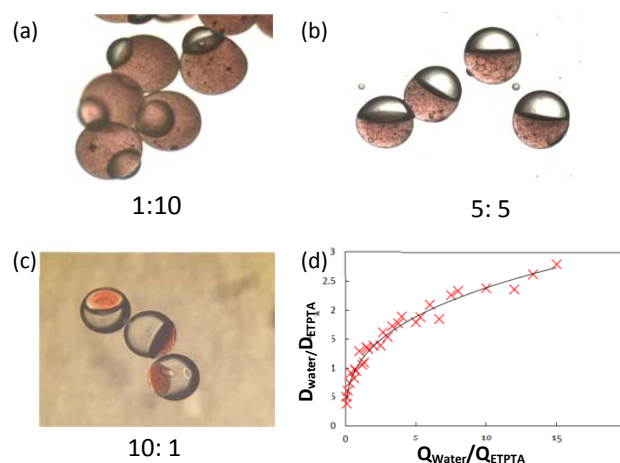
Fig. 5 The relationship of dimension ratio of Janus semi-sphere with the flow rates ratio of the corresponding fluids. a) to c) the micrographs of Janus particles with different flow rates ratio of water to ETPTA phase. a) 1:10 b) 1:1 c) 10:1 The scale bar represents 500 μm. d) the relationship of the D_{Water}/D_{ETPTA} and Q_{Water}/Q_{ETPTA}, they are positively correlated but they are not linear dependence. The red cross represent the experiment data.

Morphology control based on the change of interfacial tensions

For some application, like the catalysis field, people care the exposure area more than the volume and devote to achieving the highest exposure area of a certain phase, i.e., the highest specific area. In our work, we succeeded finding an easy way to adjust the specific area. When fixing the volumes of two phases, we find the exposure area of each phase (We take the hydrophilic phase to analyse in below description) could be highly controlled by simply changing the interfacial tensions. In our work, we adjust surfactant concentration in the continuous phase to adjust the interfacial tension between water phase and continuous phase. **Figs.** 6a~6c show the different exposure area of hydrophilic phase (black part of HHAJPs) when the surfactant (Span80) concentration is diverse. That is because the surfactant changes the interfacial tension, and then changes the contact angles between three phases. So for the same volume ratio, the encapsulation part of hydrophilic phase is different. **Fig.** 6a is the extreme case which the hydrophilic phase is almost engulfed by the other phase. And in **Fig.** 6b, the major part of hydrophilic phase is encapsulated, while in **Fig.** 6c, the minor part of hydrophilic phase is encapsulated which means the exposure area rise when the surfactant concentration increase. **Figs.** 6d and 6e elaborates how the interfacial tension change when the

surfactant concentration change. For water and liquid paraffin (continuous phase), the interfacial tension between them decrease as the Span80 concentration in the liquid paraffin increase. After the concentration increased to the critical micelle concentration (CMC), the increase of concentration don't decrease the interfacial tension. As for ETPTA and liquid paraffin (continuous phase), because they are both oil, the surfactant has scarce effect on their interfacial tension, so the interfacial tension almost stay unchanged during the whole process. **Fig.** 6e shows that the contact angles changes with the Span80 mass concentration. When neglecting the gravity (because our droplets are small), the interfacial tension would balance to zero according the Neumann's triangle at the three-phase boundary. The contact angles between each two phases are determined by interfacial tensions. Here, α represents the contact angle between water and liquid paraffin, β represents the contact angle between ETPTA and liquid paraffin, and δ represents the contact angle between water and ETPTA. γ_W represents the interfacial tension between water and liquid paraffin, γ_E represents the interfacial tension between ETPTA and liquid paraffin, and γ_{EW} represents the interfacial tension between water and ETPTA. Their schematic plot is shown in **Fig.** 6e and their relationship meets the following equation.

$$\alpha = acos[0.5(\gamma_W^2 + \gamma_{EW}^2 - \gamma_E^2)/(\gamma_W \times \gamma_{EW})] \quad (1.1)$$

$$\beta = acos[0.5(\gamma_W^2 + \gamma_E^2 - \gamma_{EW}^2)/(\gamma_W \times \gamma_E)] \quad (1.2)$$

$$\delta = acos[0.5(\gamma_E^2 + \gamma_{EW}^2 - \gamma_W^2)/(\gamma_E \times \gamma_{EW})] \quad (1.3)$$
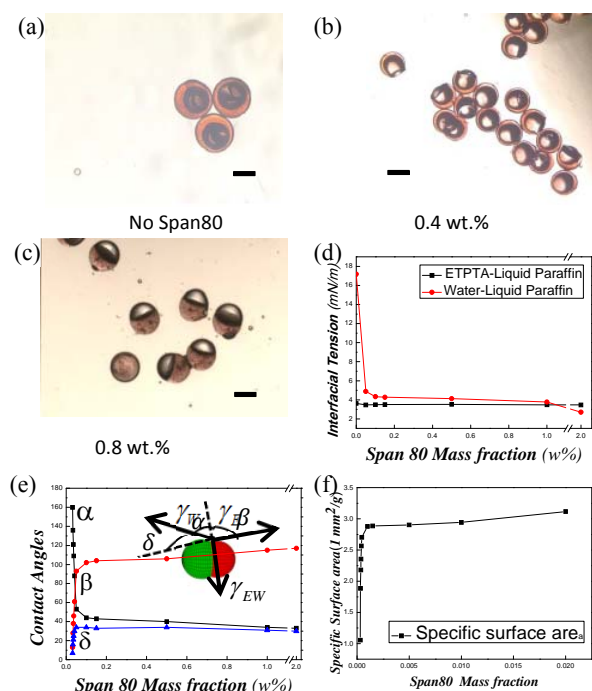

Fig. 6 The exposure surface area adjustment of hydrophilic phase. a)~c) the micrographic images of Janus droplets with the concentration of Span80 in outer phase changing from a) 0%, b) 0.4 wt.%, c) 0.8 wt.%, respectively. d)~f) show the interfacial tension, the contact angles and the specific exposure area of ETPTA

phase change with concentration of Span 80. The scale bar represents 200 μm. Hydrophilic-hydrophobic anisotropic microparticles dispersion in oil-water interface.

From **Fig.** 6e, we find that when the Span80 mass concentration increases (the interfacial tension decrease according to the **Fig.** 6d), all contact angles change, where α decrease, β and δ increase, and thus the exposure area of hydrophilic phase increases. Because the volume of water phase is fixed, after normalizing the volumes of all phases (thus the mass concentration of Span80 is transformed to mass fraction), the exposure area equals to the specific area in number. Then we draw the relationship of specific surface area of hydrophilic phase and the mass fraction of Span80. From **Fig.** 6f, we could find the specific surface area rises fast when mass fraction of Span80 increases until reaching the CMC. Such method allows us to minimize the amount of some expensive materials when keeping relatively high surface area, which is of significance in some area such as catalysis and interfacial stabilization where the exposure area determine the efficiency and volume determine the cost. High specific exposure surface area of an expensive material could always mean to be more economic.
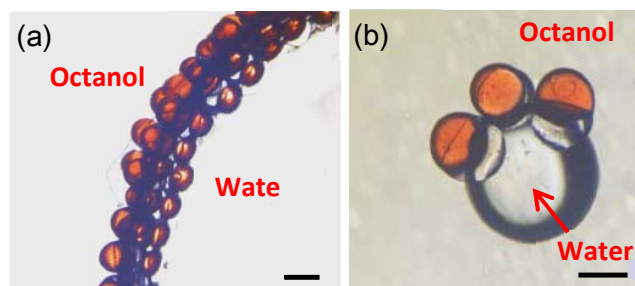

Fig. 7 The HHAJPs oriented absorbed on water-oil interface. a) many particles dispersed in the interface of octanol and water. b) several HHAJPs scattered in the surface of a water drop. The red part of the HHAJPs represent oil phase (ETPTA) and the colourless part represent water phase (PEGDA hydrogel). When dispersed on the surface, the oil phase always towards to the octanol while the water phase towards to water. The scale bar represents 200 μm.

Furthermore, we test the hydrophilic-hydrophobic property of the HHAJPs. When we put about 200 HHAJPs into a mixture of 20g octanol and 3g water and shake it for about 30 seconds, we found that all of those HHAJPs are adsorbed and directionally distributed on the oil-water interface, with the ETPTA side immersed in the octanol and the PEGDA side immersed in the water side. These particles pack closely and cover the interface, much like solid surfactant behaviour. **Fig.** 7 shows the microscopic photos of the dispersion. **Fig.** 7a shows that the particles orderly scattered in the interface. The red part represent the hydrophobic phase, and they all directs to the octanol while the other part which could be seen clearly because they are covered by the boundary of octanol and water represents hydrophilic phase and they all directs to the water. From **Fig.** 7b, we could see the dispersion of phase more clearly, it depicts three HHAJPs scatter along a water

droplet surface with the octanol environment. The red part of HHAJP (hydrophobic phase) directs to octanol while the colourless part (hydrophilic phase) directs to water. Such property of HHAJPs makes it promising in phase transfer catalysis application.

Conclusions

In summary, by RSM technology, we improved the in-situ generation of W-O Janus droplets in microfluidic device, and successfully obtained monodispersed water-oil Janus droplets and Hydrophobic-Hydrophilic Anisotropic Janus Particles. Compared with previous work, the improved method could allow much higher interfacial tension between two dispersed phases, larger volume ratio range, and larger Ca range. The size of HHAJPs could be precisely controlled. By adjusting the surfactant concentration in the continuous phase, the exposure surface area could be optimized, which allows us to use the least amount of some expensive dispersed phase to gain certain exposure area. Such HHAJPs could directionally distribute on the oil-water interface stably, indicating its potential application as interface stabilizer and phase transfer catalyst.

Acknowledgements

Notes and references

1   T. Brugarolas, B. J. Park, M. H. Lee and D. Lee, *Adv. Funct. Mater.*, 2011, 21, 3924-3931.
2   J. Faria, M. P. Ruiz and D. E. Resasco, *Adv. Synth. Catal.*, 2010, 2359-2364.
3   Y. Hu, J. Wang, C. Li, Q. Wang, H. Wang, J. Zhu and Y. Yang, *Langmuir*, 2013, 29, 15529-15534.
4   S.-H. Kim, S.-J. Jeon, W. C. Jeong, H. S. Park and S.-M. Yang, *Adv. Mater.*, 2008, 20, 4129-4134.
5   M. Marquis, D. Renard and B. Cathala, *Biomacromolecules*, 2012, 13, 1197-1203.
6   S. Seiffert, M. B. Romanowsky and D. A. Weitz, *Langmuir*, 2010, 26, 14842-14847.
7   S. N. Yin, C. F. Wang, Z. Y. Yu, J. Wang, S. S. Liu and S. Chen, *Adv. Mater.*, 2011, 23, 2915-2919.
8   Y. Chen, G. Nurumbetov, R. Chen, N. Ballard and S. A. Bon, *Langmuir*, 2013, 29, 12657-12662.
9   Y. Ning, C. Wang, T. Ngai, Y. Yang and Z. Tong, *RSC Adv.*, 2012, 2, 5510.
10 N. Prasad, J. Perumal, C.-H. Choi, C.-S. Lee and D.-P. Kim, *Adv. Funct. Mater.*, 2009, 19, 1656-1662.
11 R. K. Shah, J.-W. Kim and D. A. Weitz, *Adv. Mater.*, 2009, 21, 1949-1953.
12 X.-H. Ge, J.-P. Huang, J.-H. Xu and G.-S. Luo, *Lab Chip*, 2014, 14, 4451-4454.
13 B. Liu, J. Liu, F. Liang, Q. Wang, C. Zhang, X. Qu, J. Li, D. Qiu and Z. Yang, *Macromolecules*, 2012, 45, 5176-5184.
14 Z. Nie, S. Xu, M. Seo, P. C. Lewis and E. Kumacheva, *Langmuir*, 2010, 26, 11732-11736.
15 S. Liu, R. Deng, W. Li and J. Zhu, *Adv. Funct. Mater.*, 2012, 22, 1692-1697.
16 G. T. Vladisavljević, I. Kobayashi and M. Nakajima, *Microfluidics Nanofluidics,* 2012, 13, 151-178.
17 .J. H. Xu, H. Zhao, W. J. Lan and G. S. Luo, *Adv. Healthc. Mater.*, 2012, 1, 106-111.
18 K. Xu, J.-H. Xu, Y.-C. Lu and G.-S. Luo, *Cryst. Growth Des.*, 2013, 13, 926-935.
19 N. N. Deng, W. Wang, X. J. Ju, R. Xie, D. A. Weitz and L. Y. Chu, *Lab Chip*, 2013, 13, 4047-4052.
20 M. H. Lee, K. C. Hribar, T. Brugarolas, N. P. Kamat, J. A. Burdick and D. Lee, Adv. Funct. Mater., 2012, 22, 131-138.
21 L. Liu, W. Wang, X.-J. Ju, R. Xie and L.-Y. Chu, *Soft Matter*, 2010, 6, 3759.
22 G. T. Vladisavljević, H. C. Shum and D. A. Weitz, *Colloid. Polym. Sci.* , 2012, 115-118.
23 W. Wang, M. J. Zhang, R. Xie, X. J. Ju, C. Yang, C. L. Mou, D. A. Weitz and L. Y. Chu, *Angew Chemie*, 2013, 52, 8084-8087.
24 H. Chen, J. Li, J. Wan, D. A. Weitz and H. A. Stone, *Soft Matter*, 2013, 9, 38.
25 R. Chen, P. F. Dong, J. H. Xu, Y. D. Wang and G. S. Luo, *Lab Chip*, 2012, 12, 3858-3860.
26 W.-T. Wang, R. Chen, J.-H. Xu, Y.-D. Wang and G.-S. Luo, *RSC Adv.* 2014, 4, 16444.
27 J.-H. Xu, X.-H. Ge, R. Chen and G.-S. Luo, *RSC Adv.*, 2014, 4, 1900.
28 J. Guzowski, P. M. Korczyk, S. Jakiela and P. Garstecki, *Soft Matter,* 2012, 8, 7269.
29 S. E. Friberg, I. Kovach and J. Koetz, ChemPhysChem, 2013, 14, 3772-3776.
30 L. Ge, S. Lu and R. Guo, *J Colloid Interf. Sci.*, 2014, 423, 108-112.
31 H. Hasinovic, S. E. Friberg and G. Rong, *J Colloid Interf. Sci.*, 2011, 354, 424-426.
32 I. Kovach, J. Koetz and S. E. Friberg, *Colloid Surface A*, 2014, 441, 66-71.
33 J. Tan, J. H. Xu, S. W. Li and G. S. Luo, *Chem. Eng. J*, 2008, 136, 306-311.
34 K. Xu, C. P. Tostado, J. H. Xu, Y. C. Lu and G. S. Luo, *Lab chip*, 2014, 14, 1357-1366.
35 J. Xu, S. Li, C. P. Tostada, W. Lan and G. Luo, *Biomed Microdevices*, 2008, 2009, 243-249.
36 A. Abate, A. Poitzsch, Y. Hwang, J. Lee, J. Czerwinska and D. Weitz, *Phys Rev E*, 2009, 80.
37 Y. Zhao, Z. Xie, H. Gu, L. Jin, X. Zhao, B. Wang and Z. Gu, *NPG Asia Mater.*, 2012, 4, e25.
38 K. Xu, J.-h. Xu, Y.-c. Lu and G.-S. Luo, *Crys. Growth Des.* 2014, 14, 401-405.
39 T. Tanaka, M. Okayama, H. Minami and M. Okubo, *J. Am. Chem. Soc.*, 2005, 8058-8063.
40 C. H. Chen, R. K. Shah, A. R. Abate and D. A. Weitz, *Langmuir*, 2009, 25, 4320-4323.
41 T. Nisisako and T. Torii, *Adv. Mater.*, 2007, 19, 1489-1493.
42 W. Lan, S. Li, J. Xu and G. Luo, *Microfluid Nanofluid* 2012, 13, 491-498.
43 J. H. Xu, G. S. Luo, S. W. Li and G. G. Chen, *Lab Chip*, 2006,6,131-136..
44 B. Zhao, J. S. Moore and D. J. Beebe, *Science*, 2001, 291, 1023-1026.
45 A. Hibara, S. Iwayama, S. Matsuoka, M. Ueno, Y. Kikutani, M. Tokeshi and T. Kitamori, *Anal. Chem.*, 2005, 943-947.
46 Torza, S. & Mason, S. *Science,*1969, 163, 813.
47 Torza, S. & Mason, S. *J. Colloid Int. Sci.* ,1970,33, 67–83.